

Nanoscale

Accepted Manuscript



This is an *Accepted Manuscript*, which has been through the Royal Society of Chemistry peer review process and has been accepted for publication.

Accepted Manuscripts are published online shortly after acceptance, before technical editing, formatting and proof reading. Using this free service, authors can make their results available to the community, in citable form, before we publish the edited article. We will replace this *Accepted Manuscript* with the edited and formatted *Advance Article* as soon as it is available.

You can find more information about *Accepted Manuscripts* in the [Information for Authors](#).

Please note that technical editing may introduce minor changes to the text and/or graphics, which may alter content. The journal's standard [Terms & Conditions](#) and the [Ethical guidelines](#) still apply. In no event shall the Royal Society of Chemistry be held responsible for any errors or omissions in this *Accepted Manuscript* or any consequences arising from the use of any information it contains.



Nanoscale

ARTICLE

Layer-by-Layer Thinning of Two-Dimensional MoS₂ Film by Focused Ion Beam

Ding Wang, Yuqiu Wang, Xiaodong Chen, Yuankun Zhu*, Ke Zhan, Hongbin Cheng, Xianying Wang*

Received 00th January 20xx,
Accepted 00th January 20xx

DOI: 10.1039/x0xx00000x

www.rsc.org/

Layer-controlled two-dimensional (2D) molybdenum disulfide (MoS₂) film with tunable bandgaps is highly desired for the fabrication of electronic/photoelectronic devices. In this work, we demonstrate that Focused ion beam (FIB) can be applied to thin MoS₂ films layer-by-layer. The layer number can be controlled by simply changing the Ga⁺ beam exposure time and the thinning speed is about half layer per second. OM, AFM, PL and Raman spectra were used to monitor the change of layer numbers and characterize the morphology, thickness, and homogeneity of MoS₂ films. The FIB layer-by-layer thinning technology will establish a new methodology for rationally thinning all kinds of 2D layered materials.

Introduction

As a 2D semiconducting material, MoS₂ is attracting great attention due to its excellent optical, electrical and mechanical properties. It has numerous potential applications in catalysis, energy storage, electronic/optoelectronic devices and chemical sensors etc.¹⁻⁴ Different from graphene, MoS₂ film could be directly grown on SiO₂/Si substrates, thus it has better compatibility with the integrated circuits.⁵ Also, the bandgap of MoS₂ can be adjusted from 1.3 eV (bulk) to 1.9 eV (single layer) by changing layer numbers,⁶ and it is expected to complement or even replace graphene in electronic/optoelectronic devices. Except for the bandgaps, many other physicochemical properties are also determined by the layer number of MoS₂.⁷ For instance, enhanced photoluminescence (PL) emission with the decrease of layer number was observed, which was attributed to an indirect-to-direct bandgap transition.⁸ Wang et al. reported the piezoelectric properties of 2D MoS₂ caused by cyclic stretching and releasing of thin MoS₂ flakes were also layer number dependent. MoS₂ film with an odd layer numbers produced oscillating piezoelectric voltage and current outputs, whereas no output was observed for flakes with an even number of layers.⁹ Correlations between tunable physicochemical properties and layer number require the fabrication of "on-demand" MoS₂ films, in particular single layer MoS₂, for potential applications in electronic/optoelectronic devices.

Various strategies have been developed to fabricate MoS₂ films with certain layers, which can be generally classified into the bottom-up and the top-down technologies.¹⁰⁻¹⁵ The bottom-up approaches, including chemical vapor deposition

(CVD) and wet chemical synthesis method, are simple and inexpensive. The top-down technology achieves interlaminar stripping through physical or chemical methods such as micro-mechanical force stripping, lithium ion intercalation, and liquid ultrasonic method.¹²⁻¹⁴ However, all the methods are lacks of the control over the layer numbers, which greatly limits the application of such 2D films in nanodevices. Recently, a few novel strategies were provided to prepare thin MoS₂ films with controlled layer numbers, such as laser thinning and thermal etching etc.^{8,16} Although layer by layer thinning can be achieved by laser, the surface defect inevitably increases because of uneven energy distribution inside the laser spot. Thermal annealing method is time-consuming and lacks the control over positions, shapes etc..

Focused ion beam (FIB) is a widely used technology in sample thinning and micromachining, where high energy Ga⁺ beam is used as the bombardment source.¹⁷⁻¹⁸ By optimizing the energy of ion beam, duration, and the time of exposure, the etching speed can be finely controlled. Also, it has the flexibility to set positions, areas and shapes of the region to be processed. Thus it is expected that FIB can be used to thin MoS₂ film with controlled layer numbers, shapes etc. In this work, FIB was used to thin MoS₂ film layer-by-layer and etching conditions were investigated. FIB etched films were characterized by optical microscope (OM), Raman spectra, atomic force microscope (AFM) and Photoluminescence (PL) spectra and results show that FIB can finely control the layer number of MoS₂. It is believed that the layer-by-layer thinning technique by FIB will open up a new route to rationally fabricate 2D materials with controlled layer numbers.

Experimental

Preparation of MoS₂ films

MoS₂ film was prepared via CVD method. Before CVD growth, Mo film with the thickness of 0.5-1.5 nm was evaporated on the SiO₂/Si substrate via electron beam evaporation. The substrate was placed at the central place of tube furnace. A

College of Materials Science and Engineering, University of Shanghai for Science & Technology, Shanghai, 200093, People's Republic of China

* E-mail: xianyingwang@usst.edu.cn (Xianying Wang)

zhuyuankun@usst.edu.cn (Yuankun Zhu)

Electronic Supplementary Information (ESI) available: [details of any supplementary information available should be included here]. See DOI: 10.1039/x0xx00000x

porcelain boat containing 2.5 g sulfur was then placed in the uptake of tube furnace. The distance between the boat and substrate was kept for 10 cm. 150 sccm Argon (Ar) gas was inletted through the tube for 5-15 minutes to remove oxygen. For the MoS₂ growth, the tube furnace was heated up to 550 °C within 30 minutes. Then the temperature slowly rose to 750-850 °C within 90 minutes. Ar gas with the flow rate of 100 sccm was used as the carrier gas. The tube furnace was kept at 750-850 °C for 10 minutes and cooled to room temperature naturally. Finally, the MoS₂ film with few layers was obtained.

FIB thinning

The as-synthesized few-layer MoS₂ film was thinned by using a dual beam FIB (FEI, Quanta 3D FEG, USA) system. The precise control of the thinning process for MoS₂ thin films is mainly influenced by Ga⁺ ionic energy, Ga⁺ dose per frame, and the total amount of etched MoS₂ materials, which are respectively implemented by accelerating voltage, beam current, and thinning thickness (thinning time) in FIB setting. Therefore, in this study, the accelerating voltage, ion beam current and etching thickness are chosen as three parameters to study the FIB thinning of few layer MoS₂ films. To avoid extra exposure to the Ga⁺ ion beam, electron microscope was used for imaging while adjusting parameters, searching exact positions, etc.. Before FIB thinning, the thickness of MoS₂ layer was measured using AFM from the edge area. In order to mark the thinning zone, circles with diameter of 20 μm were etched first and the etching depth was set to be equal to the film thickness to exactly expose the initial SiO₂ surface.¹⁹ Then, the internal region of the ring was thinned by FIB with operation voltage of 10 kV and beam current intensity of 10 pA. MoS₂ films with different thicknesses were obtained by controlling the thinning time.

Characterization of materials

The morphologies of MoS₂ films were investigated via scanning electron microscope (SEM) (FEI, Quanta FEG 450, USA) and OM (Leica DL-LM, Olympus BX41, Japan). The layer number and thickness of samples were characterized by atomic force microscope (AFM) (AR, Cypher, USA). Raman spectra, Raman mapping and PL spectra measurements were carried out by using Raman Microscopy (Horiba, LabRAM HR Evolution, France) with an excitation wavelength of 532 nm. The Raman band of a Si wafer at 520.7 cm⁻¹ was used as a reference to calibrate the spectrometer. The Raman spectroscopy with 1800 lines mm⁻¹ grating has a spectral resolution better than 1 cm⁻¹. The bandgap was estimated by PL spectroscopy using He-Cd laser (325 nm) as the excitation light.

Results and discussion

3.1. Characterization of MoS₂ film

Prior to the study the FIB thinning technique, high quality MoS₂ films were first fabricated via CVD method. Fabrication conditions such as temperature, preservation time, and thickness of the Mo layer were investigated in detail. Only tiny MoS₂ flakes are observed when the reaction temperature is 750 °C. However, uniform MoS₂ film can be obtained when the reaction temperature is between 800 °C and 850 °C, indicating that the Mo film is completely sulfureted (Fig. S1). In addition, a lot of irregular MoS₂ particles or sheets on the substrate can be found when the film was grown at 850 °C, which is due to the evaporation and recrystallization of MoS₂ at high temperature. Thus, 800 °C is considered to be the appropriate reaction temperature to prepare few layer MoS₂

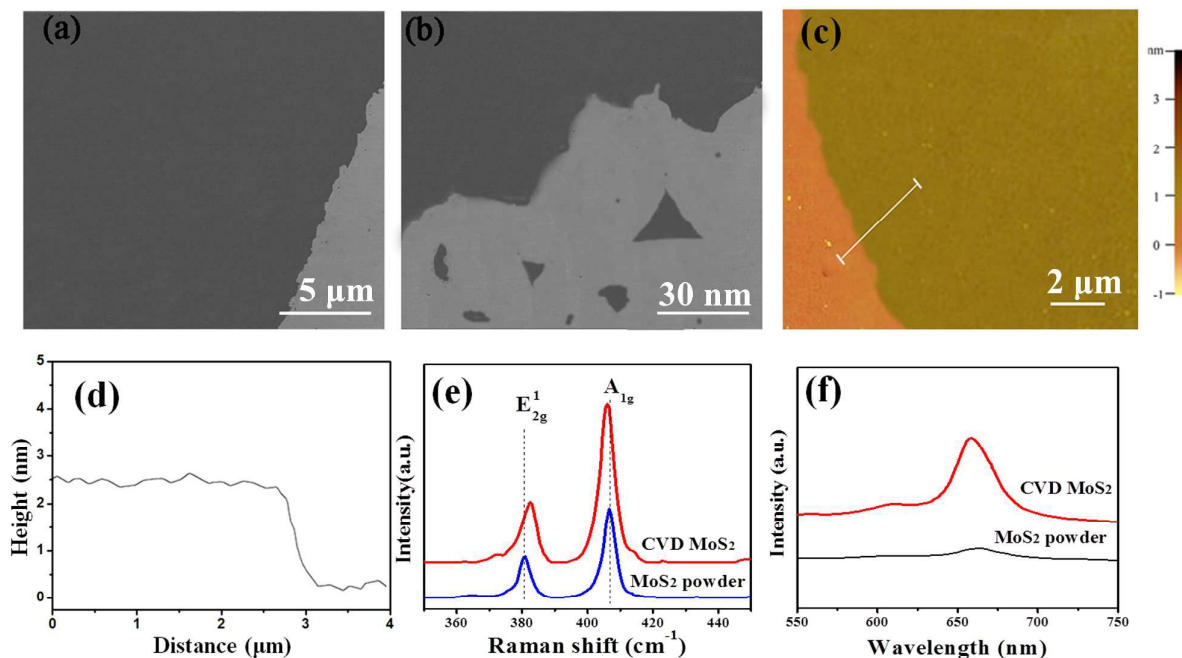


Fig. 1 (a)-(b) SEM images of MoS₂ samples obtained by CVD with low and high magnification, (c) Corresponding AFM image, (d) the thickness of 2D MoS₂ measured by AFM, (e) Raman spectra and (f) PL spectra of the MoS₂ film and the commercial MoS₂ powder.

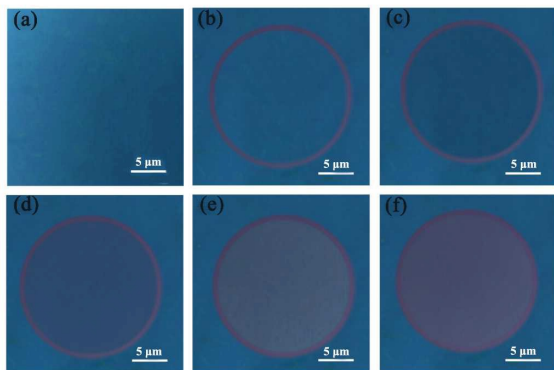


Fig. 2 The OM images of MoS₂ sample before (a) and after (b-f) thinning by FIB, with thinning time of (b) 0 s, (c) 2 s, (d) 4 s, (e) 6 s, and (f) 8 s, respectively.

films. The temperature holding time is also an important factor influencing the quality of MoS₂ films. In Fig. S2, many discontinuous sheets are observed on the surface of SiO₂/Si substrate, which is because 5 minutes is insufficient for the growth of continuous MoS₂ film. When the preservation time increases to 10 minutes, MoS₂ film is continuous and uniform. Further increased to 15 minutes will cause uneven distributions of nanoparticles on the surface. The effect of thickness of Mo film evaporated on the SiO₂/Si substrate is also studied. As shown in Fig. S3, the OM image of sample with 0.5 nm Mo film as the precursor presents discontinuous MoS₂ film. In contrast, continuous and homogeneous MoS₂ films are

obtained for the samples covered with 1 nm and 1.5 nm Mo layers. The lack of MoS₂ at the edges of SiO₂/Si substrate is due to the absence of Mo atoms in this area.

MoS₂ film prepared with the reaction temperature of 800 °C, holding time of 10 mins and Mo thickness of 1.0 nm was characterized by SEM, AFM, Raman and PL spectroscopy, and the results are shown in Fig. 1. MoS₂ (black part) evenly covers the surface of SiO₂/Si substrate (Fig. 1a). Under the enlarged view of SEM (Fig. 1b), some triangles can be seen at the edge of SiO₂/Si substrate. The triangles usually appear in the process of MoS₂ crystallization, which suggests that the process involves not only Mo atoms vulcanization but also MoS₂ recrystallization.²⁰ However, no individual triangles are found at the center part, indicating that the film is continuous. The topography and thickness of MoS₂ film were characterized by AFM under tapping mode. As shown in Fig. 1c, the film is continuous and uniform, also, the contrast between MoS₂ film and the substrate is clear. From Fig. 1d, the thickness of as-grown MoS₂ film is about 2.5 nm and the measurement error is around ± 0.2 nm. Raman and PL spectra were collected to characterize the microstructure of the as-prepared film. For comparison, the spectra of commercial MoS₂ powder were also measured. It can be seen in Fig. 1e that both the MoS₂ film prepared by CVD method and the commercial MoS₂ power present two prominent peaks including E_{2g}¹ in-plane vibration mode and A_{1g} out-plane vibration mode. The E_{2g}¹ and A_{1g} Raman peaks of the CVD sample are located at 383.4 cm⁻¹ and 406.8 cm⁻¹, with the peak distance of 23.4 cm⁻¹. Compared with that of commercial MoS₂ power (25.6 cm⁻¹), the distance

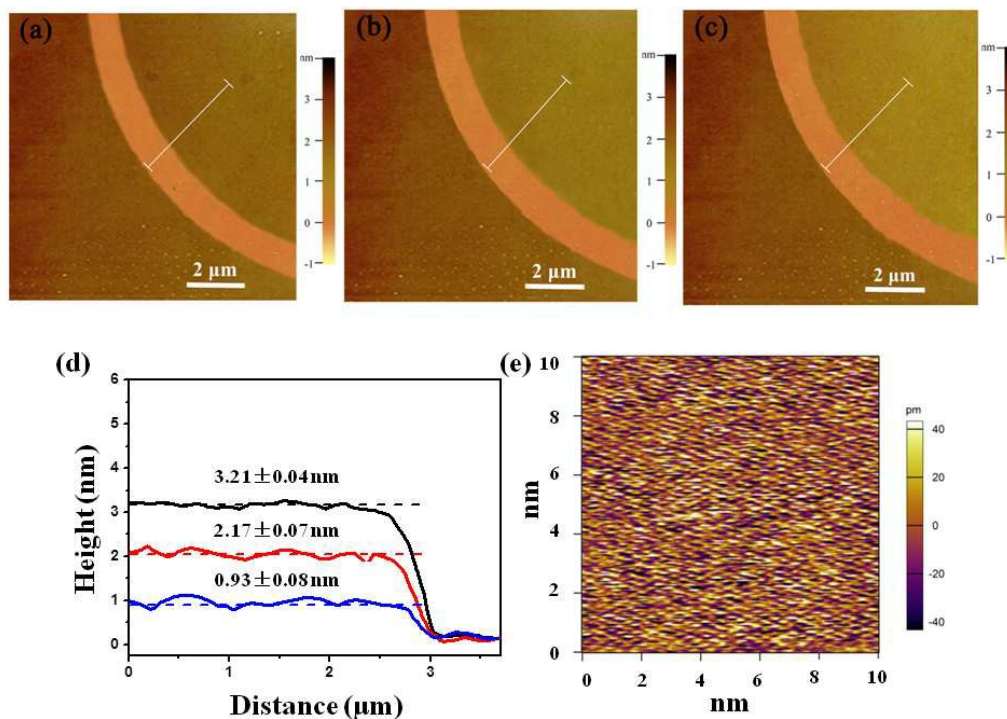


Fig. 3 AFM images of MoS₂ sample after thinning by FIB, with the thinning time of (a) 0 s, (b) 4 s and (c) 8 s, respectively, (d) the thickness of 2D MoS₂ obtained with different thinning time, (e) AFM images of MoS₂ film with high resolution.

between the two peaks is apparently narrowed. The red shift of E_{2g}^1 and blue shift of A_{1g} indicate that MoS_2 film has only few layers. As reported, PL behaviors are also closely related with the layer number of MoS_2 . Fig. 1f exhibits the PL spectra of MoS_2 film and commercial MoS_2 power. A strong emission peak at 658 nm is observed for MoS_2 film under 325 nm laser excitation. However, only very weak peak from the commercial MoS_2 power is observed. The enhanced PL performances are ascribed to an indirect-to-direct bandgap transition.²¹

To investigate the thinning capability of FIB, MoS_2 film with slightly larger thickness was fabricated. 1.5 nm Mo film was used as the precursor. The growth temperature was kept at 800 °C and the temperature holding time was set to 10 mins. The as-prepared MoS_2 film was thinned through FIB etching and processing parameters including the beam current, accelerating voltage and exposure time were investigated. Apparent color evolutions of OM images with different thinning times can be found in Fig. 2. The continuous blue area in Fig. 2a indicates that the MoS_2 film is highly uniform. As can be seen in Figs. 2b-2f, colors of thinned MoS_2 samples change from blue to violet with increasing thinning time. Variations of the colors are attributed to the reduction of light reflection, indicating the decrease of MoS_2 film thickness. The reduction of light reflection with the decrease of film thickness is due to the increased ratio of the transmitted light. The similar phenomena were also observed in other 2 D materials.^{22,23}

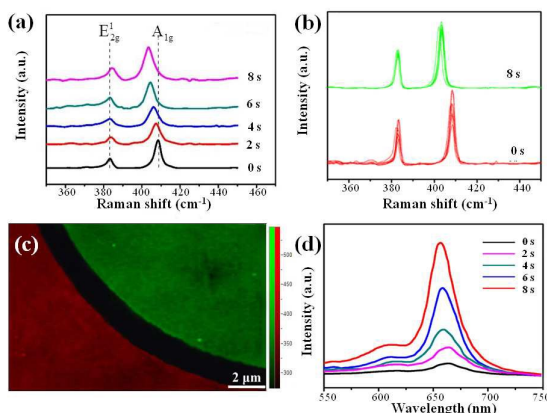


Fig. 4 (a) Raman spectra of MoS_2 sample before and after FIB thinning at different times, (b) Raman spectra and (c) Raman mapping of MoS_2 film after thinning for 8 s, (d) PL spectra of MoS_2 sample before and after FIB thinning at different time.

MoS_2 film etched for 0 s, 4 s and 8 s were further characterized using AFM and corresponding images are shown in Figs. 3a-3c. Slight color change can be observed with the increase of etching time. The topographical cross sectional profile across the scanned line in Fig. 3a-3c reveals that the thickness of the as-synthesized MoS_2 film is 3.21 ± 0.04 nm. After treatment by FIB for 4 s and 8 s, the film thickness reduce to 2.17 ± 0.07 nm and 0.93 ± 0.08 nm, respectively. Considering that the thickness of single layer MoS_2 is 0.65 nm,²¹ the corresponding layer numbers of as-grown, 4 s and 8 s FIB etched samples are 5, 3 and 1 respectively. The thinning

speed of MoS_2 is about 1 layer per 2 seconds. The enlarged view of FIB etched surface shown in Fig. 3e indicates that the film has atomic level smoothness, which is important for its usage in electronic/optoelectronic devices.

Raman spectroscopy is an effective technique for rapid identification of the thickness of MoS_2 thin films. The change of MoS_2 layer number can be identified by observing the peak positions. The separation between the two most prominent peaks E_{2g}^1 (in-plane vibration modes) and A_{1g} (out-plane vibration modes) depends on the thickness. With the decrease of layer numbers, the peak distance gradually narrowed.²⁴ The Raman spectra of MoS_2 with different thinning times are shown in Fig. 4a. As a result of the layer thickness reduction, the E_{2g}^1 and A_{1g} Raman peak of MoS_2 is redshifted and blueshifted respectively with increasing etching time.¹⁰ Raman spectra profiles taken from randomly selected pre- and post-treated regions are highly overlapped, demonstrating the uniformity of the film. As shown in Table S1, the Raman shifts of E_{2g}^1 and A_{1g} peak for 8s etched sample are 384.6 cm^{-1} and 403.1 cm^{-1} , which are in accordance with the Raman peak of single layer MoS_2 .²⁵ The results consist with the AFM characterization.

To further determine the homogeneity of FIB thinned film, Raman mapping experiment was carried out by using the confocal Raman spectroscopy. There are totally 2400 (40×60) Raman spectra collected from a $12 \mu\text{m} \times 8 \mu\text{m}$ area. By determining the Raman peak positions of the A_{1g} band, Raman mapping images can be obtained. As can be seen in Fig. 4c, the red zone represents the unetched MoS_2 film while the green zone stands for the MoS_2 film after thinning for 8 s. The homogeneous contrast of the Raman images in both the red zone and green zone indicates that layer numbers of MoS_2 film are the same in both untreated and FIB treated areas.

PL spectroscopy is also one of the most direct methods for determining the band gap of single layer MoS_2 . It is well known that bulk MoS_2 shows an indirect band gap energy of 1.3 eV,⁶ However, it gradually transforms into a direct gap semiconductor with the reduction of layer number, leading to the dramatic increase of PL emission peak.²⁶ Fig. 4d shows the PL spectra of MoS_2 after thinning for different time. A weak peak is observed at 663 nm before the FIB treatment. With the increase of thinning time, the peak becomes stronger. Also, slight blueshift can be observed. The strong PL peak observed at 655 nm from the 8 s thinned sample corresponds to the band gap of about 1.88 eV, which consists with that of single layer MoS_2 .²⁷

To precisely control the thickness of MoS_2 film and avoid possible surface damage, a very low accelerating voltage and small amount of Ga^+ dose per frame is essential. Besides, other operating parameters including the etching depths, beam spot size, overlapping rate etc. will also influence the quality of FIB processed films. Moreover, these parameters always interconnect with each other. To comprehensively understand the influence of these parameters, we carried out a series of controlling experiments. Typically, we fixed other parameters and studied the effects of accelerating voltages and beam currents. The Raman spectra and OM images of MoS_2 thin

films thinned under different accelerating voltages were shown in Fig. S4. With the increase of accelerating voltage, the intensities of the E_{2g}^1 and A_{1g} peaks decrease significantly. Under the accelerating voltages of 20 kV and 30 kV, very weak or no Raman signals can be detected, and evident damage is observed on the surface of MoS_2 films from the OM images. Thus high accelerating voltage will definitely cause damage to the samples. Fig. S5 shows the Raman spectra and OM images of MoS_2 films prepared under different beam currents of 7.7 pA, 16 pA, 48 pA and 77 pA with a constant accelerating voltage of 5 kV. With the increase of beam current, the intensities of the two prominent peaks E_{2g}^1 and A_{1g} decrease gradually, indicating gradual degradation of the crystal quality of MoS_2 film.

Conclusions

To conclude, FIB technique was successfully utilized to rationally thin MoS_2 film layer by layer. By selecting appropriate etching conditions, layer numbers of MoS_2 can be finely controlled. The thinning speed of MoS_2 is about half atomic layer per second under our experimental conditions. AFM, Raman, OM and PL characterizations collectively confirm the changes of microstructures and physical properties of MoS_2 films before and after FIB treatment. The simple, efficient and controllable FIB thinning method will have a promising future in thinning other 2D layered materials such as $MoSe_2$, WS_2 etc.. We believe that this technique will be important for obtaining high quality 2D films with one or few atomic layers for device applications.

Acknowledgements

This work was supported by the National Natural Science Foundation of China (51402192, 51572173 and 11402149), Natural Science Foundation of Shanghai (14ZR1428000), State Key Laboratory of Heavy Oil Processing (SKLHOP201503), Shanghai Talent Development Funding and the Hujiang Foundation of China (B14006).

Notes and references

- 1 K. S. Novoselov, A. K. Geim, S. V. Morozov, D. Jiang, Y. Zhang, S. V. Dubonos, I. V. Grigorieva, A. A. Firsov, *Science*, 2004, **306**, 666.
- 2 H. L. Zeng, X. D. Cui, *Chemical Society Reviews*, 2015, **44**, 2629.
- 3 M. Chhowalla, Z. F. Liu, H. Zhang, *Chemical Society Reviews*, 2015, **44**, 2584.
- 4 X. Huang, Z. Zeng, H. Zhang, *Chemical Society Reviews*, 2013, **42**, 1934.
- 5 Y. Zhan, Z. Liu, S. Najmaei, P. M. Ajayan, J. Lou, *Small*, 2012, **8**, 966.
- 6 P. Joo, K. Jo, G. Ahn, D. Voiry, H. Y. Jeong, S. Ryu, M. Chhowalla, B. S. Kim *Nano Letters*, 2014, **14**, 6456.
- 7 H. Thomas, *Accounts of Chemical Research* 2015, **48**, 65.
- 8 A. Castellanos-Gomez, M. Barkelid, A. M. Goossens, V. E. Calado, H. S. J. Van der Zant, G. A. Steele, *Nano Letters* 2012, **12**, 3187.
- 9 L. Wang, Y. L. Li, F. Zhang, L. Lin, S. M. Niu, D. Chenet, X. Zhang, Y. F. Hao, T. F. Heinz, J. Hone, Z. L. Wang, *Nature*, 2014, **514**, 470.
- 10 X. Ling, Y. H. Lee, Y. X. Lin, W. J. Fang, L. L. Yu, M. S. Dresselhaus, J. Kong, *Nano Letters*, 2014, **14**, 464.
- 11 K. K. Amara, L. Q. Chu, R. Kumar, M. L. Toh, G. Eda, *Applied Materials* 2014, **2**, 092509.
- 12 H. Li, Z. Y. Yin, Q. Y. He, H. Li, X. Huang, G. Lu, D. W. H. Fam, A. L. Y. Tok, Q. Zhang, H. Zhang, *Small*, 2012, **8**, 63.
- 13 A. A. Jeffery, C. Nethravathi, M. Rajamathi, *The Journal of Physical Chemistry C*, 2014, **118**, 1386.
- 14 Emily. P. Nguyen, B. J. Carey, T. Daeneke, J. Z. Ou, K. Latham, S. Zhuiykov, K. Kalantar-zadeh, *Chemistry of Materials*, 2015, **27**, 53.
- 15 H. Q. Wang, K. Kalantar-Zadeh, A. Kis, J. N. Coleman, M. S. Strano, *Nature Nanotechnology*, 2012, **7**, 699.
- 16 J. Wu, H. Li, Z. Y. Yin, J. Q. Liu, X. H. Cao, Q. Zhang, H. Zhang, *Small*, 2013, **9**, 3314.
- 17 C. Li, L. R. Zhao, Y. F. Mao, W. G. Wu, J. Xu, *Scientific Reports*, 2014, **5**, 8236.
- 18 W. X. Li, A. Cui, C. Z. Gu, P. A. Warburton, *Microelectronic Engineering*, 2012, **98**, 301.
- 19 X.Y. Wang, S. F. Xie, J. Liu, S. O. Kucheyev, Y. M. Wang, *Chemistry of Materials*, 2013, **25**, 2819.
- 20 Y. M. Shi, H. N. Li, L. J. Li, *Chemical Society Reviews*, 2015, **44**, 2744.
- 21 A. Splendiani, L. Sun, Y. B. Zhang, T. Li, J. Kim, C. Y. Chim, G. Galli, F. Wang, *Nano Letters*, 2010, **10**, 1271.
- 22 C. Ruppert, O. B. Aslan, T. F. Heinz, *Nano Letters*, 2014, **14**, 6231.
- 23 H. Li, Q. Zhang, C. C. R. Yap, B. K. Tay, T. H. T. Edwin, A. Olivier, D. Baillargeat, *Advanced Functional Materials*, 2012, **22**, 1385.
- 24 R. Ganatra, Q. Zhang, *ACS Nano*, 2014, **8**, 4074.
- 25 M. Buscema, G. A. Steele, H. S. J. Van der Zant, A. Castellanos-Gomez, *Nano Research*, 2014, **7**, 561.
- 26 G. Eda, H. Yamaguchi, D. Voiry, T. Fujita, M. W. Chen, M. Chhowalla, *Nano Letters*, 2011, **11**, 5111.
- 27 P. Joo, K. Jo, G. Ahn, D. Voiry, H. Y. Jeong, S. Ryu, M. Chhowalla, B. S. Kim, *Nano Letters*, 2014, **14**, 6456.